

Supplemental Material

A Source for Mesoscopic Quantum Optics

Georg Harder¹, Tim J. Bartley^{1,2}, Adriana E. Lita², Sae Woo Nam², Thomas Gerrits², and Christine Silberhorn¹

¹*Integrated Quantum Optics Group, Applied Physics,*

University of Paderborn, 33098 Paderborn, Germany and

²*National Institute of Standards and Technology, 325 Broadway, Boulder, CO 80305, USA*

(Dated: October 19, 2015)

CORRELATION FUNCTIONS

Correlation functions, first introduced by Glauber [1], are one way to characterize photon number statistics. For example, varieties of nonclassicality criteria can be constructed based on second and higher order moments of the electromagnetic field [2, 3]. Such criteria identify nonclassical fields directly from the measured statistics in a loss tolerant way without complicated analysis techniques and have been utilized with low order correlation functions [4, 5]. Having access to higher order correlation functions gives a more complete description of the underlying photon number statistics and increases the possibilities in characterizing quantum states. For example, exotic quantum states might only reveal their nonclassicality when higher order correlations are included. In this section we show that we are able to calculate these higher order correlation functions.

We focus on correlation functions of the form $g^{(n)} = \frac{\langle a^{\dagger n} a^n \rangle}{\langle a^\dagger a \rangle^n}$ for one mode or $g^{(m,n)} = \frac{\langle a^{\dagger m} a^m b^{\dagger n} b^n \rangle}{\langle a^\dagger a \rangle^m \langle b^\dagger b \rangle^n}$ for two modes, where a , a^\dagger and b , b^\dagger are the usual annihilation and creation operators. They can be calculated from photon number probabilities p_k using $\langle a^{\dagger n} a^n \rangle = \sum_k k \prod_{l=0}^{n-1} (k-l) p_k$.

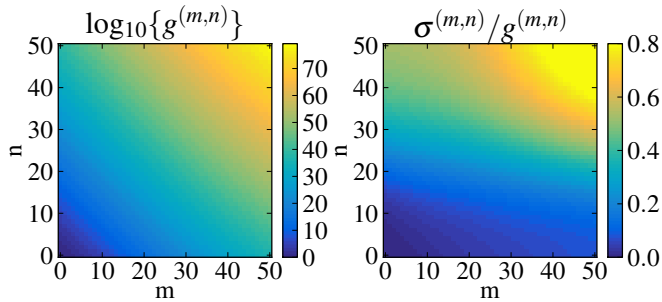


FIG. 1. Left: $g^{(m,n)}$ for the state with $\langle n \rangle = 20$. Right: Relative error obtained from a Monte-Carlo simulation based on the measured probability distribution. Values up to $g^{(40,40)}$ seem reliable. The asymmetry in the two modes arises from asymmetric detection efficiencies.

In fig. 1 we show the two mode $g^{(m,n)}$ for the bright state $\langle n \rangle = 20$. We estimate the uncertainties of the values by performing a simple Monte-Carlo simulation: Based on the measured photon number probabilities, we draw measurement frequencies from $8.2 \cdot 10^6$ events

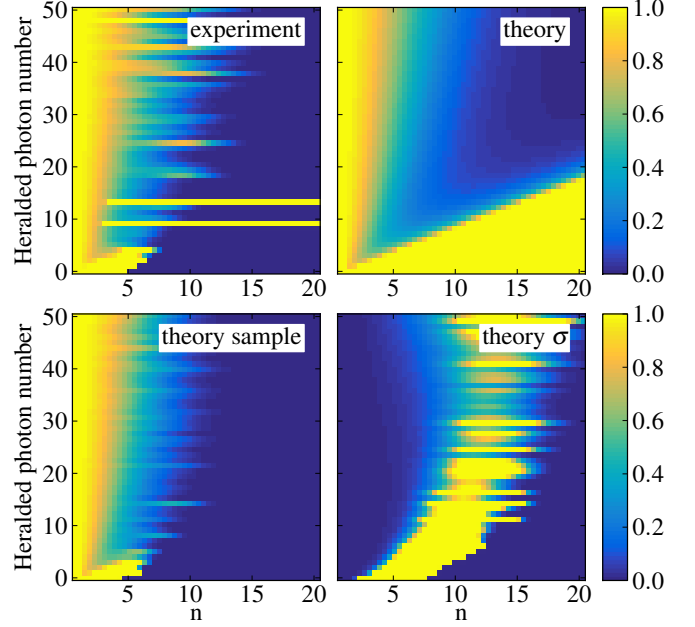


FIG. 2. Correlation functions $g^{(n)}$ for heralded states from a PDC state with $\langle n \rangle = 7$. Top: Comparison of experiment and theory. Bottom left: Simulation with $8.2 \cdot 10^6$ events. Bottom right: Expected standard deviation from a Monte-Carlo simulation. Only the region left of the yellow area is reliable with the given statistics.

and calculate the according correlation functions. From 10000 such trials, we calculate the standard deviations. Values up to $g^{(40,40)}$ seem to have reasonably low values.

In fig. 2 we show $g^{(n)}$ values for heralded states from the PDC state $\langle n \rangle = 7$. For the error analysis, we perform the same Monte-Carlo simulation, though this time based on theoretical probability distributions, due to relatively low numbers of heralded events for higher photon numbers. For example, the 35-photon herald happens only about 1000 times. This is one reason, why the statistical uncertainties dominate already above $g^{(10)}$. However, the general agreement with theory is very good. Almost all values are significantly below one, which is the bound for classical states.

NONCLASSICALITY

Following [3], we construct the correlation matrix

$$M = \begin{pmatrix} \langle : \hat{f}_1^\dagger \hat{f}_1 : \rangle & \langle : \hat{f}_1^\dagger \hat{f}_2 : \rangle & \cdots & \langle : \hat{f}_1^\dagger \hat{f}_N : \rangle \\ \langle : \hat{f}_2^\dagger \hat{f}_1 : \rangle & \langle : \hat{f}_2^\dagger \hat{f}_2 : \rangle & \cdots & \langle : \hat{f}_2^\dagger \hat{f}_N : \rangle \\ \vdots & \vdots & \ddots & \vdots \\ \langle : \hat{f}_N^\dagger \hat{f}_1 : \rangle & \langle : \hat{f}_N^\dagger \hat{f}_2 : \rangle & \cdots & \langle : \hat{f}_N^\dagger \hat{f}_N : \rangle \end{pmatrix},$$

where $\vec{f} = (1, \hat{n}_a, \hat{n}_b, \hat{n}_a^2, \hat{n}_a \hat{n}_b, \hat{n}_b^2, \dots, \hat{n}_b^N)$, $\hat{n}_a = a^\dagger a / 2$, $\hat{n}_b = b^\dagger b / 2$ and $: : \hat{f}_i^\dagger \hat{f}_j :$ denotes normal ordering. If M has at least one negative eigenvalue, the state is nonclassical. This condition is fulfilled for all states presented here. To estimate the uncertainties, we again apply a Monte-Carlo simulation. In the best case, for the $\langle n \rangle = 7$ state, the lowest eigenvalue has a significance of more than 100 standard deviations. This shows the high quality of the measured statistics.

LOSS INVERSION

To get a glimpse of how our states would look without losses, we fit a model to the data. The model consists of a state that can be described as a mixture of a (spectrally) multimode PDC state, a coherent state and a thermal state:

$$\rho = \rho_{\text{PDC}}(n^{\text{PDC}}, K) \otimes \rho_\alpha(n_s^\alpha, n_i^\alpha) \otimes \rho_{\text{th}}(n_s^{\text{th}}, n_i^{\text{th}}), \quad (1)$$

where n are the respective mean photon numbers and K the effective mode number of the PDC state. We expect K to be low since the marginal $g^{(2)}(0)$ measurements mentioned in the paper suggest $K \approx 1.13$. We hence choose exponentially decaying coefficients λ_k^2 for each (spectral) mode, whereas $\sum_k \lambda_k^2 = 1$ and $K = 1 / \sum_k \lambda_k^4$ [6, 7]. The squeezing parameters for each (spectral) PDC mode are given by $r_k = B \lambda_k$, where B is the overall optical gain. Such exponentially decaying coefficients are a reasonable approximation for low effective mode numbers.

The losses are described by a standard beam splitter model with transmissions η_s and η_i in the two beam paths. The photon number probabilities are given by $p_{kl}^{\text{out}} = \sum_{mn} L_{km}^s(\eta_s) L_{ln}^i(\eta_i) p_{mn}^{\text{in}}$, and $L_{kn}(\eta) = \binom{n}{k} \eta^k (1-\eta)^{n-k}$. In eq. 1, the photon number distributions of the three contributions are independent. That means that the total photon number distribution p^{in} is a convolution of the three individual distribution. This can be implemented numerically in a straight forward way.

Finally, we minimize the weighted sum of the least square differences

$$\sum_{mn} ((p_{mn}^{\text{meas}} - p_{mn}^{\text{out}}) / \sigma_{mn})^2, \quad (2)$$

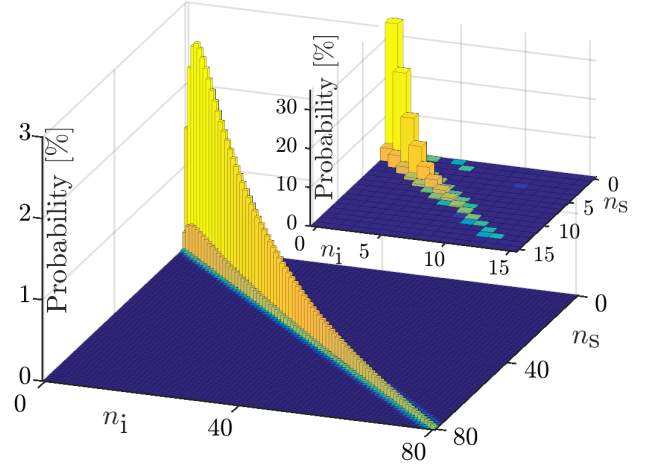


FIG. 3. Inferred states before losses. a) High power state ($\langle n \rangle = 20$) using a parameter fit to the data. b) Low power state ($\langle n \rangle = 1.4$) using full loss inversion without assumptions about the state.

where p_{mn}^{meas} are the measured photon number probabilities, p_{mn}^{out} the probabilities of the expected state after losses and $\sigma_{mn} = 1/N + \sqrt{p_{mn}^{\text{meas}}/N}$ estimates for the statistical error due to N total events. Effectively, this is a fit with eight parameters ($\eta_s, \eta_i, n_{\text{PDC}}, K, n_s^\alpha, n_i^\alpha, n_s^{\text{th}}, n_i^{\text{th}}$). Allowing Poissonian and thermal background statistics covers most optical and electrical background signals while keeping the number of free parameters very low.

The fit result for the state with $\langle n \rangle = 20$ is shown in fig. 3 and has the fit parameters

η_s	43.13(3)%
η_i	52.12(4)%
n^{PDC}	20.30(2)
K	1.097(1)
n_s^α	0.14(12)
n_i^α	0.38(5)
n_s^{th}	0.00(12)
n_i^{th}	0.00(5)

The fidelity with the data is 99.98%. The largest contribution in photon number by almost two orders of magnitude is the PDC. Furthermore, the effective mode number is low in agreement with the $g^{(2)}(0)$ measurements.

We can also regard such a fit as an efficiency estimation that is not impacted by non-PDC counts. In the case of our more efficient two-TEs setup configuration with the $\langle n \rangle = 7$ state, it suggests efficiencies of 64% and 68%.

For comparison, we perform a general loss inversion [8] for a low power state with $\langle n \rangle = 1.4$, shown in fig. 3 (inset), restricting the space to < 15 photons. Again, the inverted state resembles the expected PDC state very well. The number of free parameters is very high ($15^2 - 1$ in

this example) such that general loss inversion becomes infeasible for states with higher mean photon numbers.

METHODS: TRACE ANALYSIS

Each detection event of the TES is a voltage pulse $V(t)$ whose shape depends on the detected photon number. The characteristics of these traces are different for each TES and the photon numbers cannot be well distinguished by peak height alone. However, good photon number resolution can be obtained by simply using the average trace as a template $\bar{V}(t)$ and take the overlap $\int dt V(t)\bar{V}(t)$ to distinguish between photon numbers[9]. This method is ideal if the shapes of all pulses are similar and works well for coherent input light. In our case, however, the full range of photon numbers is present and the shapes are different for high and low photon numbers. We therefore adapt this technique as follows: We calibrate the TES responses using coherent input light. For 20 different input power settings, we calculate the average traces $\bar{V}_i(t)$ and calibrate the overlaps of each based on the Poissonian photon number expectations. Since Poissonian distributions are relatively narrow, this calibration is only reliable around the respective mean photon numbers. Then, for an unknown detection event, we calculate the overlaps with 20 templates giving 20 photon number estimations, ideally all the same, and take that particular estimation that is closest to the mean photon number of its template. This method extends the range over which we can reliably resolve photon number as compared to the one-template approach and even gives reliable estimations of photon numbers beyond the single-photon resolution regime. The clustering of the overlaps can still be seen up to 20 photons in a histogram, allowing for cross checking the calibration simply by counting peaks. To estimate systematic uncertainties in the $g^{(2)}(0)$ results of fig. 3, we rescale all templates slightly until the photon numbers are clearly over- or underestimated giving a worst case (or maximum range) effect of our photon number estimate on $g^{(2)}(0)$.

1367-2630, .

- [8] A. Feito, J. S. Lundeen, H. Coldenstrodt-Ronge, J. Eisert, M. B. Plenio, and I. A. Walmsley, *New J. Phys.* **11**, 093038 (Sep. 2009), ISSN 1367-2630, .
- [9] Z. H. Levine, T. Gerrits, A. L. Migdall, D. V. Samarov, B. Calkins, A. E. Lita, and S. W. Nam, *J. Opt. Soc. Am. B* **29**, 2066 (Aug. 2012), .

-
- [1] R. J. Glauber, *Phys. Rev.* **130**, 2529 (Jun. 1963), .
 - [2] W. Vogel, *Phys. Rev. Lett.* **100**, 013605 (Jan. 2008), .
 - [3] A. Miranowicz, M. Bartkowiak, X. Wang, Y.-x. Liu, and F. Nori, *Phys. Rev. A* **82**, 013824 (Jul. 2010), .
 - [4] M. Avenhaus, K. Laiho, M. V. Chekhova, and C. Silberhorn, *Phys. Rev. Lett.* **104**, 063602 (Feb. 2010), .
 - [5] J. Sperling, M. Bohmann, W. Vogel, G. Harder, B. Brecht, V. Ansari, and C. Silberhorn, *Phys. Rev. Lett.* **115**, 023601 (Jul. 2015), .
 - [6] J. H. Eberly, *Laser Phys.* **16**, 921 (Jun. 2006), ISSN 1054-660X, 1555-6611, .
 - [7] A. Christ, K. Laiho, A. Eckstein, K. N. Cassemiro, and C. Silberhorn, *New J. Phys.* **13**, 033027 (Mar. 2011), ISSN